Article

A Fractal Description of Fluvial Networks in Chile: a Geography not as Crazy as Thought

Francisco Martinez [1,*,‡], Hermann Manriquez [2,‡], Alberto Ojeda [1,†,‡] and Gabriel Olea [1,†,†,‡]

[1] Escuela de Ingenieria Civil, Pontificia Universidad Catolica de Valparaiso, Chile; francisco.martinez@pucv.cl,[†] alberto.ojeda.w@gmail.com, [†,†] oleagabrielt@hotmail.com
[2] Instituto de Geografia, Pontificia Universidad Catolica de Valparaiso, Chile; hermann.manriquez@pucv.cl
* Correspondence: francisco.martinez@pucv.cl (FM)
‡ These authors contributed equally to this work.

Abstract: Chilean geography is highly variable, not only from a climatic and hydrological point of view, but also a morphological one, showing unpredictable natural patterns with marked contrasts throughout the country, for which sometimes it is considered as a "crazy" geography. In this paper we have investigated this apparent disorganized character by exploring the fractal properties of fluvial networks extracted from basins distributed across the continental territory. Analytical and semi-empirical methods were applied, finding striking patterns of organization in the distributions of Horton parameters and the fractal dimension of the drainage networks. Fractal dimension reveals to be quite dependent on the drainage area of each unit, showing clear groupings by tectonic and climatological factors. Such dimension reveals to be an important geomorphic parameter, if not the only one able to capture the real morphology of a fluvial network. From our results and despite the diversity of landforms, hydrological, climatic and tectonic conditions, Chilean's geography is perhaps not as crazy and disorganized as believed.

Keywords: fluvial networks ; Chilean's watersheds ; monofractal dimension ; morphometry ; structural control.

1. Introduction

Fractals are objects whose geometrical structure remains invariant regardless of the observation scale [1]. These objects can be found in different scientific areas such as medicine, physics, mathematics, geology, biology and particularly, in geomorphology where many natural systems can be described by using fractal concepts, for example the shape of relief, borderlines of lakes, coasts and rivers and particularly, the topology of streams networks [1–4]. In contrast to other classical metrics introduced for basins (see *e.g.* [5]), fractal dimension arises as a revolutionary geomorphic index able to capture the geometrical complexity of drainage patterns observed over the landscape. Such dimension can be interpreted as the topological dimension where such invariability remains [1,6]. To reach this state of knowledge, the collection and measuring of real networks in different environments is a fundamental task to explore the variability, coherence, and validity of such dimension.

Benjamin Subercaseux wrote a popular book about Chile [7], describing the territory as a "crazy", and sometimes unpredictable, geography emphasising the significant variability of topographical, climate and even, folk characteristics observed along the continent. In this context, Chilean fluvial networks arise as an interesting example of application of estimation of the mono-fractal dimension of such systems. The aim of the present article is to explore this apparent "crazy" character applying a fractal geometrical analysis to estimate the fractal degree of stream networks extracted from different watersheds of the country at different observation levels. Particular emphasis was put on exploring the connections between this parameter and the tectonics and morphometric features of the relief.

Preprints (www.preprints.org) | NOT PEER-REVIEWED | Posted: 29 December 2021 doi:10.20944/preprints202112.0471.v1

Horton [8] pioneered on this topic introducing a quantitative description of streams developed in a fluvial network. Considering a hierarchical ordering of the streams, Horton defined the following set of ratios representing such development [9]:

$$R_{B,\omega} = \frac{N_{\omega-1}}{N_\omega} \quad R_{L,\omega} = \frac{L_\omega}{L_{\omega-1}} \quad R_{A,\omega} = \frac{A_\omega}{A_{\omega-1}} \tag{1}$$

where $R_{A,\omega}, R_{B,\omega}$ and $R_{L,\omega}$ denote the area, bifurcation and length ratios of the streams, respectively. The parameters L_ω, N_ω and A_ω correspond to the length and number of drains of the sub-catchments of area A_ω, where $\omega = 2, ..., \Omega$ is the order of the streams, whose maximum value is Ω [9]. An striking observation from Horton is that for high enough dense networks, the parameter $R_{q,\omega}$ shows almost convergent values. Such observation can be interpreted, *a priori*, as an intimate connection between fractals and self-similar trees [10,11]. These convergent values can be well represented by the average of each ratio, let's say $R_q = \frac{1}{\Omega}\sum_{\omega=1}^{\Omega} R_{q,\omega}$, for $q = A, B, L$. The ratios R_A, R_B, R_L can be considered characteristic parameters for a given fluvial network.

Inspired on Hack's law [12], Mandelbrot explored this connection showing that $l \propto A^{d/2}$, where A is the area of catchment, $d \approx 1.1$ the meandering fractal dimension and l the length of the mainstream, respectively. Based on this relation and assuming the constancy of the drainage density across the network, Feder [6] improved this definition proposing the relationship $d = 2ln(R_L)/ln(R_B)$. Rosso et al. [13] extended this result suggesting the law $d = max(1, 2ln(R_L)/ln(R_A)$, in agreement with the topological minimum path dimension deduced by Liu [14].

1.1. Fractal dimension of a fluvial network

One of the problems of previous formulations is the need of connecting them with the fractal dimension of the entire network. La Barbera and Rosso [2] derived a law for this situation, assuming that Horton parameters holds through the whole network across different scales:

$$D_1 = \frac{ln(R_B)}{ln(R_L)} \; if \; R_B > R_L \quad \& \quad D_1 = 1 \; if \; R_B < R_L \tag{2}$$

According to [2], Eq.2 leads to values in the range $1.5 < D_1 < 2.0$ (1.67 in average). The authors argued about the impossibility of reaching values close to 2, car fluvial networks show decreasing drainage densities for increasing contributing areas. Tarboton et al.[15] states that [2] assumes that mainstreams identify with topological objects of dimension 1. However, many real streams show meandering patterns where $d \neq 1$. Tarboton et al. [15] proposed the following law to estimate the fractal dimension in this situation:

$$D_2 = d\frac{ln(R_B)}{ln(R_L)} \tag{3}$$

Tarboton et al. argues that there exists large evidence showing that $d \approx 1.14$, limiting Eq.3 to values in the range $D_2 < 2$ ([3,15,16]) . This is coherent with observations made at larger scales where it is reasonable to assume that streams drain each point of the basin as pointed by [17]. In an interesting exchange, La Barbera and Rosso [18] refuted the conclusion of Tarboton proposing a modification of Eq.3 as follows:

$$D_3 = \beta\frac{ln(R_B)}{ln(R_L)} \tag{4}$$

where $\beta = \frac{1}{2-d}$. Also from a theoretical point of view, Liu [14] worked with infinite dense networks ($\Omega \to \infty$), at both meso and microscale. The author proposed five different dimensions associated to the structure of individual streams, one of them related to the fractal dimension of whole the network. Such dimension can be estimated from the next relationship:

Preprints (www.preprints.org) | NOT PEER-REVIEWED | Posted: 29 December 2021 doi:10.20944/preprints202112.0471.v1

$$D_4 = 2\frac{ln(R_B)}{ln(R_A)} \tag{5}$$

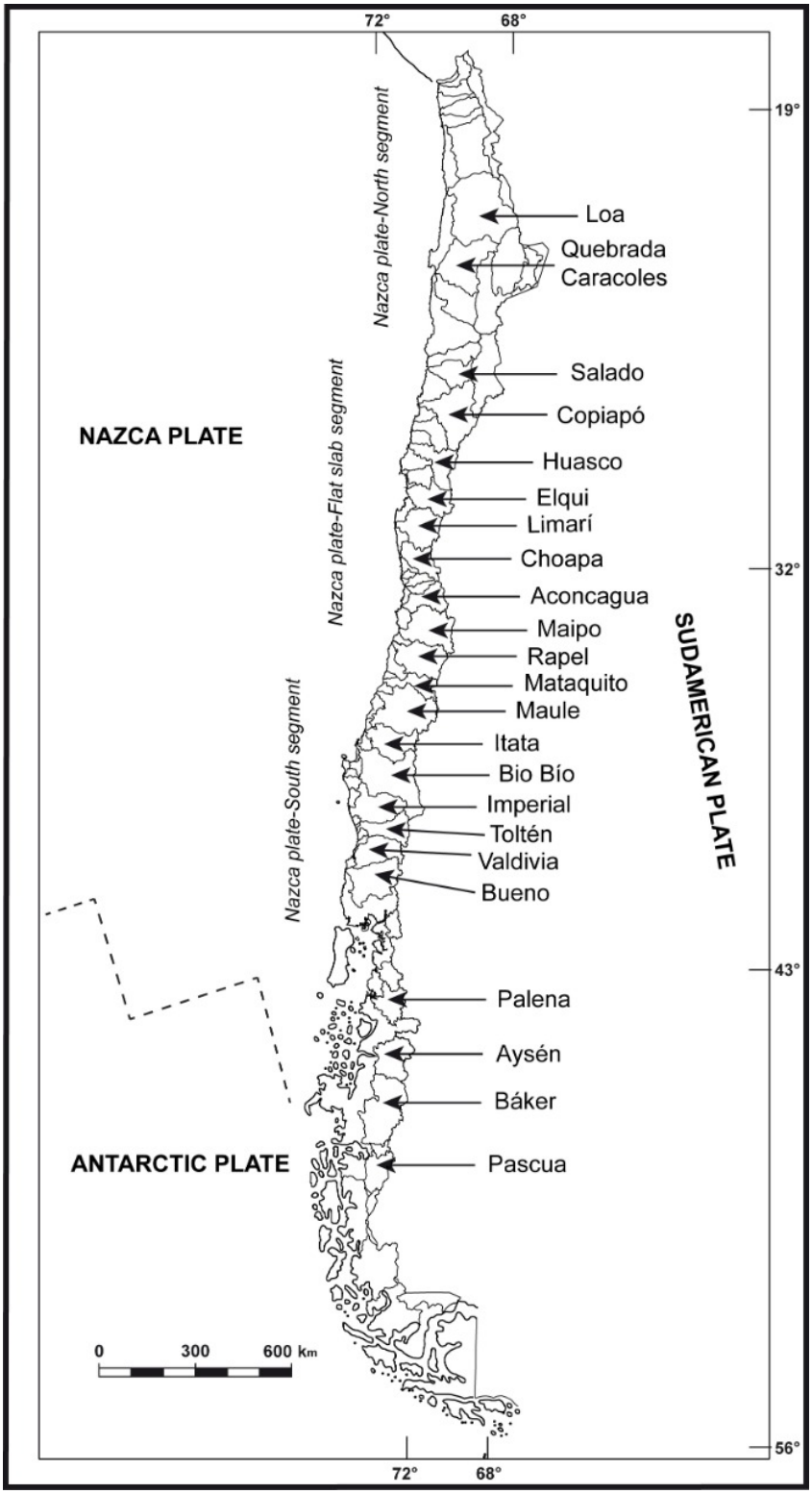

Figure 1. Localization of the 23 basins used in the present study. The tectonic segments of Chilean territory, ordered from north to south, can be also observed.

Preprints (www.preprints.org) | NOT PEER-REVIEWED | Posted: 29 December 2021 doi:10.20944/preprints202112.0471.v1

Although Eqs.2-5 shows to be a practical approach to describe the fractal dimension of stream networks, they requires a huge amount of geographic information to obtain the morphometric parameters. On the other side, there are several limitations of these methods that deserves to be considered. One of them is related with the self-similarity hypothesis. This assumption has been objectively refuted by Kirchner [19]), giving rise to another approaches based on self-affine attributes of networks [17,20–23]. This self-affine character naturally arises from the morphological anisotropy of the network and the combination of the different tectonic processes that constrains the diffusion of the streams over the time ([24]).

2. Methodology

2.1. Determination of the fractal dimension and geomorphic indexes

In this study, the determination of the mono-fractal dimension of the networks was conducted by following two different approaches. The first method is based on Horton metrics and its invariance laws, allowing to estimate the fractal dimension according to Eqs.2-5 (see Section 1.1). The second method is more practical in our opinion, based on the application of a box-counting algorithm with the software *Fractalyse*. This empirical method does not requires the determination of Horton ratios and/or any other morphometric parameter of the basin. Fractalyse software was developed at THEMA Laboratory and it can be applied to determine fractal patterns in different kind of networks, urban and natural [25,26]. This software was fed with Landsat-5 satellite images obtained from NASA's platform site. Every image was first analysed by using image processing tools in Matlab, from which the planar structure of the network can be extracted. Inspired on the concept of topological recovering of a surface, a given drainage pattern can be covered by a finite set of $N(s)$ squared-box of side s. The parameter s can be reduced step by step, increasing the number of boxes covering the figure. According to Rodriguez-Iturbe and Rinaldo [27], the fractal dimension of the network arising from this method can be calculated from the next relationship:

$$D_F = \lim_{s \to 0} \frac{log(N(s))}{log(\frac{1}{s})} \tag{6}$$

In order to compare the morphological characteristics of each network, we have also estimated some geomorphic parameters typically used to describe the characteristics of drainage basins [5]. This is, the shape index F, the circularity index C and the elongation factor E, respectively:

$$F = \frac{A}{L^2}, \quad C = \frac{4\pi A}{P^2}, \quad E = \frac{2\sqrt{A}}{\sqrt{\pi} L} \tag{7}$$

where L is a characteristic length of the watershed (usually the longest distance of the basin) and P its perimeter. We also introduce the drainage density (ρ) of the network. This parameter is provided by GRASS-GIS and defined as follows:

$$\rho = \frac{Z}{A} \tag{8}$$

2.2. Definition of the region of interest

In the present report we have analyzed 23 large-basins, located between the latitudes $17°30'S$ and $56°30'S$, covering a total area of $363,354 km^2$. The area of each network is larger than $10,000 km^2$ and they were delimited by following the guidelines proposed by *Direccion General de Aguas (DGA)*, a governmental agency focused on water resources management. Figure 1 shows the location of these units from north to south. From our point of view, this classification considers reasonably well the tectonic, geographic and climatic diversity of the country. The geographical analysis of every basin was conducted on the software GRASS-GIS. This software provides the Horton ratios R_A, R_B, R_L, the

Preprints (www.preprints.org) | NOT PEER-REVIEWED | Posted: 29 December 2021 doi:10.20944/preprints202112.0471.v1

hierarchical order Ω, catchment and sub-catchments drainage areas A, the average slope i_m and the mean elevation (H_m) of each network. The order Ω was determined by following the criteria proposed by Strahler [28]. These parameters are presented in Table 1.

Table 1. Morphometric parameters of large-basins ordered from north to south and by tectonics influence. (*NPN*: Nazca plate-north, *NPFS*: Nazca plate-flat slab,*NPS*: Nazca plate-south, *AP*: Antarctic plate). Here A is the drainage area, i_m the mean slope, H_m the mean elevation of the unit and Ω the maximum order of each network according to Strahler's hierarchical ordering. Drainage density and geomorphic indexes were also included. (The superscript $()^*$ denotes the basins chosen for analysis at sub-basin level).

Tectonics	Basin	$A(km^2)$	$i_m(\%)$	$H_m(m)$	Ω	F	C	E	$\rho(km^{-1})$
NPN	**Loa*(LO)**	51056	13	2401	9	1.88	0.40	0.27	1.86
	Caracoles (QC)	32537	9	1947	10	0.84	0.43	0.33	2.15
	Salado (SA)	16826	20	3086	9	0.28	0.33	0.19	1.55
	Average					**1.00**	**0.38**	**0.26**	**1.85**
NPFS	Copiapo (CO)	18608	33	2707	8	0.49	0.34	0.24	1.16
	Huasco (HU)	9759	43	2738	7	0.40	0.31	0.25	0.98
	Elqui*(EQ)	9484	46	2520	7	0.47	0.34	0.26	0.99
	Limari (LI)	11650	37	1673	7	0.62	0.45	0.30	1.02
	Choapa (CHO)	7815	39	1701	7	0.46	0.33	0.29	1.02
	Aconcagua (AC)	7341	42	1847	7	0.37	0.37	0.24	1.20
	Average					**0.47**	**0.36**	**0.26**	**1.06**
NPS	Maipo (MP)	14810	37	1664	8	0.49	0.38	0.25	1.28
	Mataquito (MAT)	6219	31	1106	7	0.20	0.22	0.18	1.13
	Rapel (RA)	14041	33	1166	8	0.44	0.39	0.27	1.21
	Maule (MA)	14788	17	432	8	0.57	0.34	0.24	1.17
	Itata (IT)	11457	19	581	8	0.40	0.34	0.27	1.17
	Bio Bio (BB)	24223	24	805	8	0.28	0.30	0.22	1.06
	Imperial (IM)	13443	15	397	7	0.44	0.42	0.24	1.09
	Tolten (TO)	8100	22	555	7	0.39	0.35	0.20	1.15
	Valdivia*(VA)	11470	23	489	7	0.49	0.39	0.28	0.96
	Bueno (BU)	13897	19	422	8	0.46	0.40	0.30	1.12
	Palena (PAL)	11584	41	865	8	0.49	0.20	0.24	1.00
	Aysen (AY)	12781	36	834	7	0.62	0.35	0.29	1.01
	Average					**0.44**	**0.34**	**0.25**	**1.11**
AP	**Baker*(BA)**	29326	31	891	8	0.88	0.37	0.23	1.06
	Pascua (PA)	12141	31	943	8	0.54	0.31	0.20	1.06
	Average					**0.71**	**0.34**	**0.22**	**1.06**

In order to explore the fractal properties of the basins at a finer scale, a sub-set of 30 sub-basins were extracted from Loa, Elqui, Valdivia and Baker basins (ordered in north-south direction). The same analysis detailed before was applied to each of these units, in order to obtain the individual fractal structure and morphometric properties of their drainage networks. In this context, eight sub-basins were extracted from Loa network ($LO1 - LO8$),seven sub-basins were extracted from Elqui network ($EQ1 - EQ8$); from Valdivia network seven more ($VA1 - VA7$) and finally, seven sub-basins from Baker network ($BA1 - BA7$). To the best of our knowledge, only [29] has conducted previous studies about morphometric properties of Chilean northern basins, although limited to a few units located between *Pampa Colorada* and *Pampa Tamarugal*. Instead, the analysis presented in this study takes is more extended along the territory. The main characteristics of these sub-networks can be observed in Table 2.

Preprints (www.preprints.org) | NOT PEER-REVIEWED | Posted: 29 December 2021 doi:10.20944/preprints202112.0471.v1

Table 2. Morphometric parameters of large basins, with A the drainage area, i_m the mean slope, H_m the mean elevation of the unit and Ω the maximum order of the network according to Strahler's hierarchical ordering. Geomorphic indexes were also included and the drainage density, as well.

Basin	Sub-basin	$A(km^2)$	$i_m(\%)$	$H_m(m)$	Ω	F	C	E	$\rho(km^{-1})$
Loa	LO1	120	6.17	974	9	0.24	0.23	0.56	1.21
	LO2	122	4.50	980	9	0.19	0.26	0.49	1.29
	LO3	7551	7.51	1985	9	0.36	0.25	0.68	2.21
	LO4	8017	8.70	3800	9	0.26	0.19	0.57	1.70
	LO5	311	4.89	1181	9	0.33	0.26	0.65	1.81
	LO6	616	8.30	1663	9	0.24	0.29	0.55	2.88
	LO7	469	5.57	1489	9	0.17	0.25	0.47	2.83
	LO8	3208	5.49	2170	9	0.37	0.21	0.69	2.51
	Average					**0.27**	**0.24**	**0.58**	**2.05**
Elqui	EQ1	1073	15.80	1027	7	0.32	0.23	0.64	1.05
	EQ2	737	18.81	1634	7	0.36	0.28	0.67	1.02
	EQ3	4086	25.48	3527	7	0.29	0.18	0.60	0.91
	EQ4	563	18.57	1052	7	0.26	0.20	0.58	0.97
	EQ5	261	22.16	1666	7	0.20	0.20	0.51	1.03
	EQ6	131	20.93	1368	7	0.21	0.29	0.52	1.23
	EQ7	51	21.42	1481	7	0.37	0.32	0.69	1.59
	EQ8	1515	27.15	3202	7	0.28	0.28	0.60	0.97
	Average					**0.29**	**0.25**	**0.60**	**1.10**
Valdivia	VA1	3367	8.31	215	7	0.15	0.18	0.43	1.09
	VA2	1486	13.76	630	7	0.19	0.22	0.50	1.10
	VA3	1386	18.81	997	7	0.37	0.16	0.68	0.99
	VA4	316	10.94	220	7	0.20	0.20	0.50	1.03
	VA5	615	9.29	200	7	0.28	0.23	0.60	1.01
	VA6	107	6.61	207	7	0.21	0.32	0.51	1.14
	VA7	960	11.76	447	7	0.29	0.23	0.61	0.11
	Average					**0.24**	**0.22**	**0.55**	**0.92**
Baker	BA1	1896	20.33	874	8	0.14	0.19	0.43	0.96
	BA2	3197	17.66	934	8	0.15	0.16	0.44	1.06
	BA3	394	27.62	1282	8	0.22	0.21	0.53	0.87
	BA4	306	14.68	898	8	0.09	0.28	0.34	1.00
	BA5	4785	8.32	870	8	0.40	0.31	0.72	1.16
	BA6	386	19.61	1061	8	0.30	0.25	0.62	0.91
	BA7	1499	18.82	1126	8	0.19	0.18	0.49	1.12
	Average					**0.22**	**0.23**	**0.51**	**1.01**

3. Results

3.1. About the Drainage Patterns

Figure 2 shows the drainage patterns obtained in large-basins. The geometry of these units respond to the action of both, the slope and landscape's organization. Such organisation traduces on three main morphostructural bands: the *Cordillera de los Andes*, the *Central Depression* and the *Cordillera de la Costa*. These bands contribute to shape the drainage patterns observed on every network, where the *dendritic* pattern is the dominant feature of the networks in the country as observed in Figure 2 and Appendix A, showing a clear east-west runoff direction. This pattern is generated on relatively homogeneous lithological substrates with similar resistance properties to hydrodynamic erosion and where the tributaries connect at acute angles ($< 90°$). Looking with more detail, drainage patterns taking grid or rectangular shapes can be also observed, a clear sign of structural control on streams diffusion. Moreover, the runoff regime of the networks occurs in the east-west direction and the largest units develops over the three morphostructural bands. On the other hand, the characteristics of the drainage patterns of sub-basins can be observed in Appendix A.

Preprints (www.preprints.org) | NOT PEER-REVIEWED | Posted: 29 December 2021 doi:10.20944/preprints202112.0471.v1

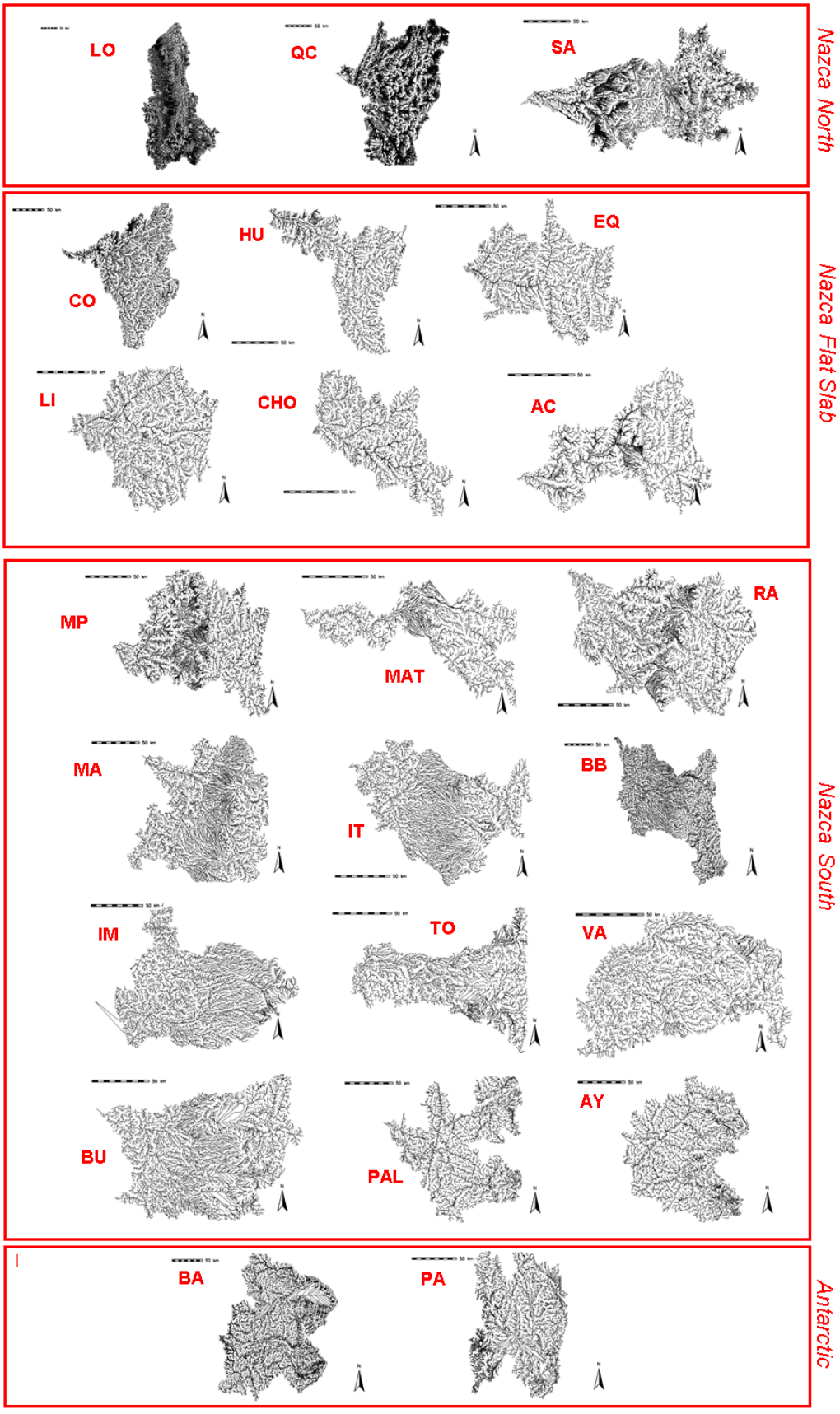

Figure 2. Fluvial networks of large basins obtained from GRASS-GIS, ordered from north to south. Units were sorted by tectonic plate influence and every image is in its proportional areal dimensions (scale 1:50,000).

 doi:10.20944/preprints202112.0471.v1

Fault macro-systems also help to delimit these morphostructural bands. The Atacama Fault Zone in the north and Liquiñe - Ofqui Fault Zone in the south (the most important fault systems in Chile), separate the coastal and andean units from the central depression [30,31]. The mountainous units are constituted by different types of rocks, this is, volcanic, volcanoclastic, intrusive and sedimentary rocks [32]. A different scenario takes place in the central depression where sedimentary rocks has been deposited by fluvial, glacial, alluvial and volcanic processes, developing from east to west. These deposits have contributed to their filling and plainform appearance.

Then, to characterize the geometry of drainage basins just looking at their patterns and drainage density is not enough, justifying the use of new parameters taking into account this variability. Loa, Caracoles and Salado basins in the north plate show high drainage densities, this is, $\rho = 1.86, 2.15, 1.55 km^{-1}$, respectively. The index F is quite variable too, falling in the range $0.28 \leq F \leq 1.88$. The average slopes of these units also falls in the range $9\% \leq i_m \leq 20\%$, which are particularly high. The northern networks develop mainly over the Central Depression in a hyper-arid climate context and under the tectonic influence of the northern zone of the Nazca plate. Their drainage patterns are essentially dendritic (from LO to SA in Figure 2) although, in the Salado basin (SA) the influence of the Central Depression begins to disappear. Here, part of the basin develops on mountainous sectors and rectangular patterns are also locally observed.

The basins located between the Copiapo and Aconcagua rivers (CO to AC in Figure 2) are quite similar both in their network patterns and their drainage density. They develop mainly on the mountainous reliefs where the Central Depression has started to disappear and to fall into the influence area of the flat subduction of the Nazca Plate (*Nazca Flat Slab*). For these units, the networks clearly organize around a main stream and the drainage pattern is once again dendritic, especially in that regions of the Central Depression. However, there is a clear trend to adopt lattice patterns in the mountains regions of the Cordillera de los Andes and the Cordillera de la Costa. There, the smaller streams connect to the higher ones at almost 90°. These characteristics traduce in quite homogeneous drainage densities fluctuating in the range $0.98 \leq \rho \leq 1.20 km^{-1}$ and $0.37 \leq F \leq 0.62$. The mean slopes for these units are particularly high with values in the range $33\% \leq i_m \leq 46\%$.

Basins between the regions of Maipo and Aysen (MP to AY in Figure 2) locates to the south of Nazca Plate. They develop in a Mediterranean climate with marked seasonality and under a rainfall regime. In this region, the drainage pattern and density shows a clear the influence of the aforementioned morphostructural units. This influence traduces in north-south strip's arrangement. In almost all the cases, a dendritic drainage pattern is observed again over the Central Depression and also over mountain regions. Lattice and rectangular patterns can be also observed with tributaries bifurcating rather at almost right angles. It is interesting to note that in the Itata basin (IT), a parallel pattern develops very well in the Central Depression. This case corresponds to a large fluvio-alluvial fan associated with the Laja river sub-basin, formed from successive dam breaks of volcanic materials from the Quaternary. Here the shape index falls in the range $0.20 \leq F \leq 0.62$ and $\rho \approx 1.0$, showing a maximum of 1.28 in the extreme north of this plate (for MP) and 0.96 in the south of this plate (for VA).

In Austral and Patagonian regions, Palena and Aysen basins (BA and PA in Figure 2) are under the tectonic influence of the Antarctic plate, developing over the Cordillera de Los Andes. A common drainage pattern here is the parallel and trellis one, where acute contact angles between tributary streams are practically nonexistent. For this reason, the structural control of these networks is mainly related to an intense faulting of the crust and the aggressive erosive process existent from the Quaternary glaciations. The temperate climate of this region provides abundant rainfall conditions throughout the year. These characteristics strongly influence the runoff regime of rivers, many of them torrential with high flow rates. For these networks the mean slope $i_m \approx 31\%$ (very high) and the drainage densities are also particularly high, showing values in the range

Preprints (www.preprints.org) | NOT PEER-REVIEWED | Posted: 29 December 2021 doi:10.20944/preprints202112.0471.v1

$1.87 \leq \rho \leq 2.49$. The morphological parameters of each network are summarized in Table 2.

Thus, in average the shape index (F) is very different between large-networks, although this is not the case of C and E, both of them showing no significant variation from one network to another. However, dramatic differences arise for these parameters at sub-basin level. In this case, F is not only more homogeneous, but its values strongly decreases in the range $0.22 \leq F \leq 0.29$. Similar values are observed respect to C. However, the parameter E shows a significant increase falling into the range $0.51 \leq E \leq 0.60$. All of these indexes shows a dramatic departure from the values reported in Table 1. A similar conclusion can be deduced with respect to ρ. Despite the similar order of the watersheds (Ω), the differences between Tables 1-2 are non-negligible.

3.2. About the Distribution of Horton Ratios

Figure 3a-3c shows the frequency distributions of Horton ratios for all the fluvial networks (23 large-networks and 30 sub-networks). A first look at each distribution shows that the peaks of frequency are reached at different ratios, that is, $R_A = 5.25, R_B = 5.25, R_L = 3.75$ for large-networks and $R_A = 6.25, R_B = 5.75, R_L = 4.25$ in sub-networks. Notice that the distribution related to R_B shows similarities in both cases as observed in Figure 3b.

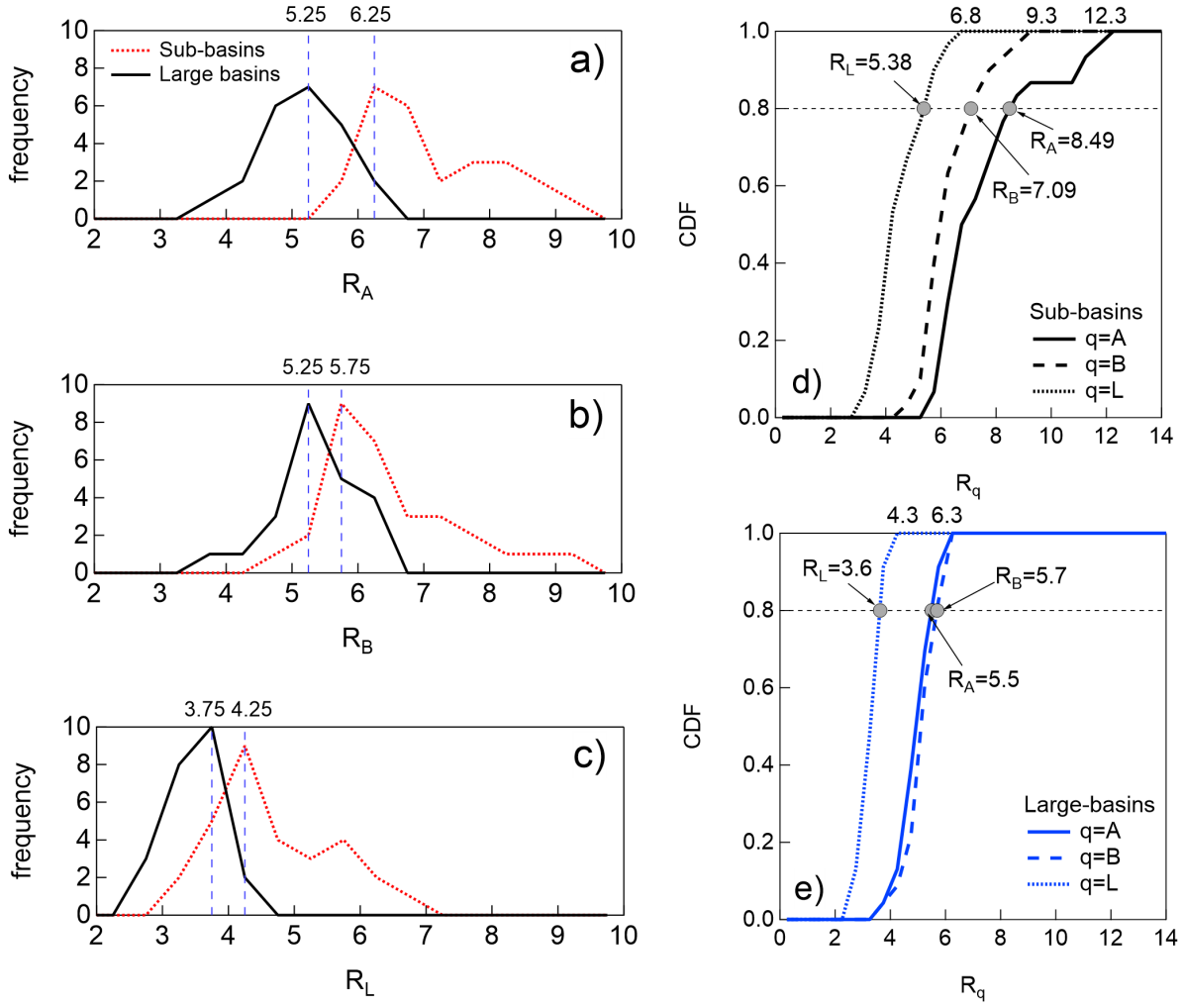

Figure 3. (**a**)-(**c**) Frequency distribution of R_A, R_L, R_B for large-networks (continuous line in black) and sub-networks (pointed-lines in red). The peaks of each draw were included for reference; (**d**) and (**e**) CDF curves for the Horton ratios, for large and sub-networks. Horizontal dashed-line corresponds to $CDF = 80\%$.

Preprints (www.preprints.org) | NOT PEER-REVIEWED | Posted: 29 December 2021 doi:10.20944/preprints202112.0471.v1

Figure 3d-3e shows the Cumulative Normalized Frequency Distribution (CDF) of the Horton ratios. Once again, important differences arise on these curves depending on the size of the network. A referential value was included in these last two figures just to emphasise such differences (see the horizontal dashed lines). Respect to this last point, Figures 3d-3e show that Horton ratios saturate around $R_A = 8.49, R_B = 7.09, R_L = 5.38$ at sub-basins level, and around $R_A = 5.5, R_B = 5.7, R_L = 3.6$ when dealing with large-basins. Almost all the curves shows also an almost constant growth-rate, but their mean slopes depend upon the size of the network. The constancy of each slope can be interpreted *a priori* as a sign of a certain homogeneity on the diffusion of streams into watershed. Unexpectedly, only R_A presents a secondary outbreak for very large ratios.

On the other hand, Figure 4 shows the distribution of R_A, R_B, R_L versus $log(A)$ (the logarithm of the area) for all the measurements. Points in the range $1.7 \leq log(A) \leq 3.8$ correspond to sub-networks and those in the range $log(A) \leq 3.8$ correspond to large-networks. Scattering bands of $\pm 50\%$ were also drawn around each mean fit to emphasise the significant dispersion of measurements. Surprisingly, each distribution shows a decreasing behaviour that can be reasonably fitted by a linear function of negative slope η (as indicated in Figure 4). Notice that η values are quite similar between R_L and R_B ($= -0.90$ and -0.87, respectively), but quite different respect to R_A for where $\eta = -1.87$, almost the double.

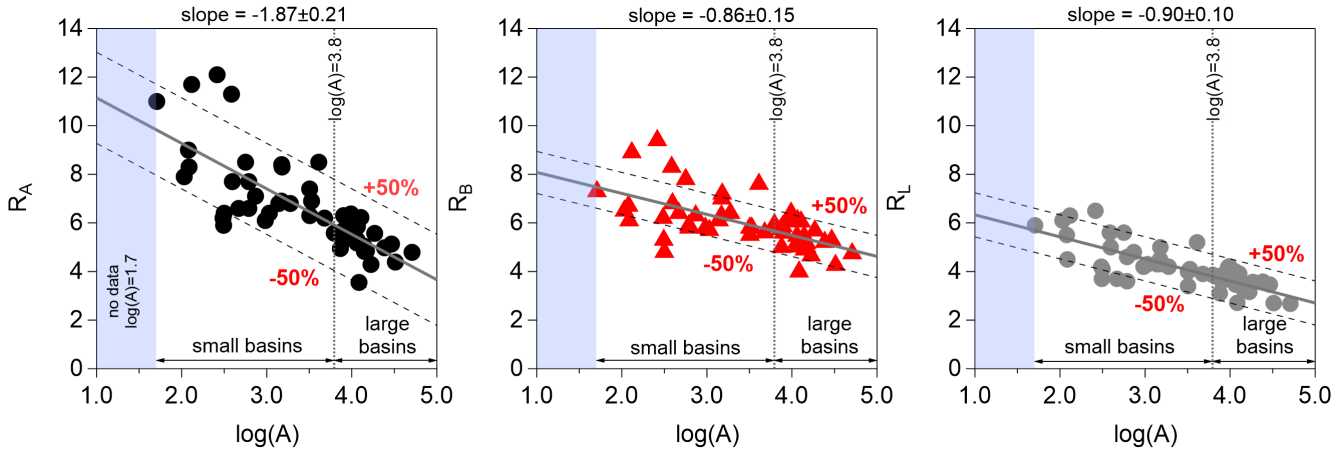

Figure 4. Comparison between the averaged Horton ratios R_q versus $log(A)$, with $q = A, B, L$. The continuous line is the mean fit for each curve of approximated slope $\eta = -1.87 \pm 0.21, -0.90 \pm 0.10, -0.86 \pm 0.15$ for $q = A, L, B$. A $\pm 50\%$ scattering band was traced around each fit as a guide to the eye.

3.3. Fractal Dimension of Networks

In this section the interplay between the fractal dimension and some morphological properties of the networks is explored. Table 3 shows the fractal dimension of each network calculated from Fractalyse, ordered by tectonic segment's influence. If we look at the values obtained only for large basins, we readily note that networks located at Nazca North plate-segment show the highest values of the entire record. In particular, the overall fractal dimension for Loa network is $D_F \approx 1.89$, the highest value of the present study. However, the fractal dimension of networks under the influence of Nazca Flat Slab plate decreases into the range $1.51 \leq D_F \leq 1.72$. The units influenced by Nazca South plate shows a clear homogeneity in the distribution of D_F, showing values bounded into the range $1.50 \leq D_F \leq 1.71$, very close to the results observed in the last situation. However, when we reach the networks located at Austral-Patagonian regions, the fractal dimension increases again leading to the values $D_F = 1.63$ for Pascua network and $D_F = 1.71$ for Baker. Thus, clear differences arise depending on the tectonic segment influencing basin's topography, suggesting that fractal dimension is a parameter controlled at some point by tectonic processes and, to a lesser degree, by erosive-related

Preprints (www.preprints.org) | NOT PEER-REVIEWED | Posted: 29 December 2021 doi:10.20944/preprints202112.0471.v1

phenomena. This point of view is in agreement with the interpretation of the fractal dimension proposed by some authors for fluvial networks (*e.g.* [24,33]).

Table 3. Fractal dimension D_F for large basins and its sub-basins obtained from Fractalyse. Loa, Elqui, Valdivia and Baker basins have been marked in red.

Tectonics	Basin	Sub-basin	D_F	Tectonics	Basin	Sub-basin	D_F	Tectonics	Basin	Sub-basin	D_F
NPN	Loa		1.89	NPS	Maipo		1.63	AP	Baker		1.71
		LO1	1.37		Mataquito		1.50			BA1	1.47
		LO2	1.38		Rapel		1.58			BA2	1.56
		LO3	1.71		Maule		1.63			BA3	1.30
		LO4	1.64		Itata		1.59			BA4	1.31
		LO5	1.43		Bio Bio		1.71			BA5	1.59
		LO6	1.55		Imperial		1.58			BA6	1.30
		LO7	1.51		Tolten		1.55			BA7	1.46
		LO8	1.75		Valdivia		1.50		Pascua		1.63
	Quebrada Caracoles		1.87			VA1	1.53				
	Salado		1.66			VA2	1.49				
	Copiapo		1.72			VA3	1.47				
	Huasco		1.56			VA4	1.30				
	Elqui		1.51			VA5	1.33				
		EQ1	1.49			VA6	1.24				
		EQ2	1.45			VA7	1.45				
		EQ3	1.51		Bueno		1.56				
		EQ4	1.36		Palena		1.55				
NPFS		EQ5	1.27		Aysen		1.56				
		EQ6	1.26								
		EQ7	1.29								
		EQ8	1.45								
	Limari		1.55								
	Choapa		1.53								
	Aconcagua		1.68								

From data presented in Table 3, we have built the curves shown in Figure 5. Figure 5a compares the fractal dimension D_F with the mean slope of each network ($log(i_m)$ for simplicity); sub-basin data was also included. Although, not clear trends can be observed between the points, most of measurements obtained from large-basins fall into a high-sloped region. However, when analysing sub-basin data it is quite surprising that sub-networks extracted from Loa ($LO1 - LO8$) falls in a sloping regime different from that measured for the entire basin LO (low-slope vs. high-slope). A similar situation is observed for the case of Elqui (EQ), Valdivia (VA) and Baker (BA) basin. Such differences indicate that morphometric properties analysed at a finer radius of observation present significant departure from those obtained from the large-basins containing them. A large sub-set of measurements falls into a moderated slope region, constituting a transition-like region between low and high-sloped networks. On the other side, Figure 5b compares D_F with the drainage density ρ. In this case most of points concentrate into the region $0.8 \leq \rho \leq 1.24$; only $VA7$ gets-out of it. In this region, D_F shows a wide variation, going from 1.20 to 1.67 and no reasonable fitting function seems reasonable. However, into the range $\rho > 1.24$ fractal dimension shows a slight growth for increasing values of ρ leading to values closer to $D_F = 1.89$ (LO large-basin). Notice that most of fractal values in the range $\rho > 1.24$ are under the influence of Nazca North plate-segment.

Preprints (www.preprints.org) | NOT PEER-REVIEWED | Posted: 29 December 2021 doi:10.20944/preprints202112.0471.v1

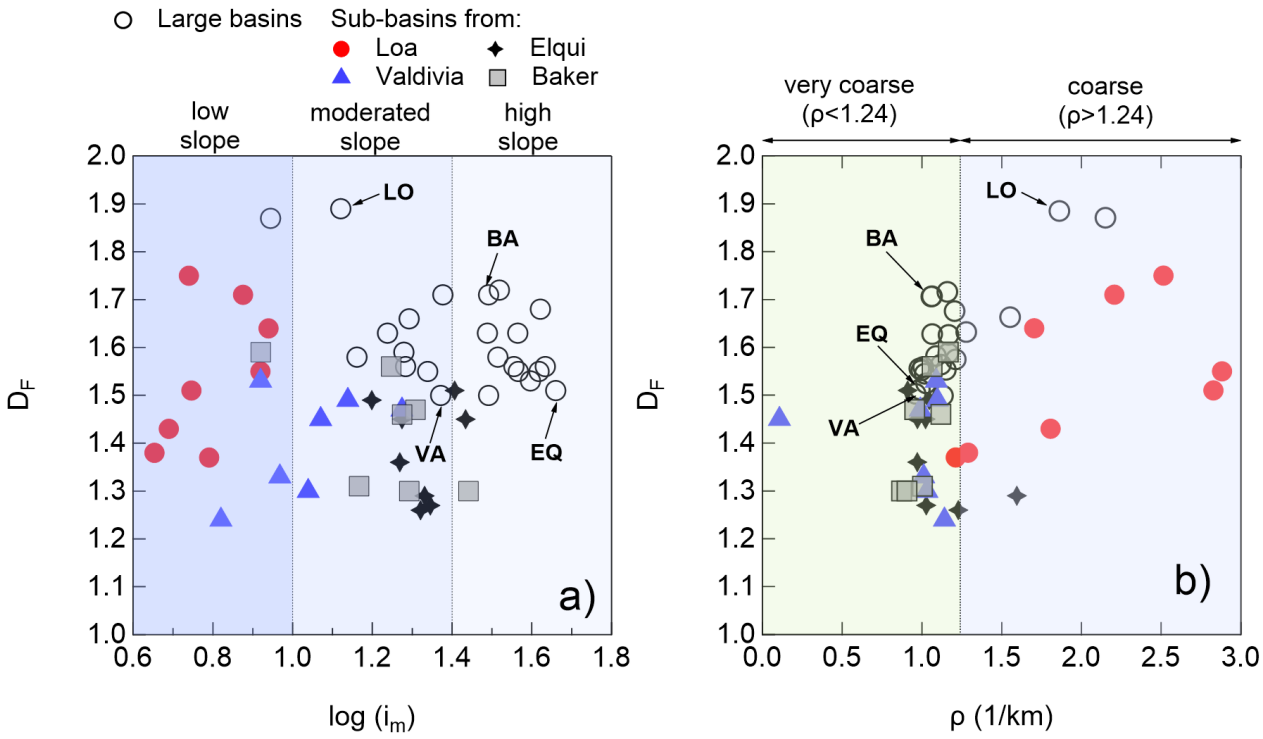

Figure 5. Fractalyse results versus (**a**) the slope of each basin and (**b**) versus the drainage density ρ. In (**a**) three regions were drawn to separate the slope regimes from low to high. In (**b**) two regions were drawn, one for $\rho \leq 1.24$ (very coarse drainage networks) and another one, for $\rho > 1.24$ (coarse drainage networks). Loa, Elqui, Valdivia and Baker basins were indicated to remark the differences between large and sub-networks.

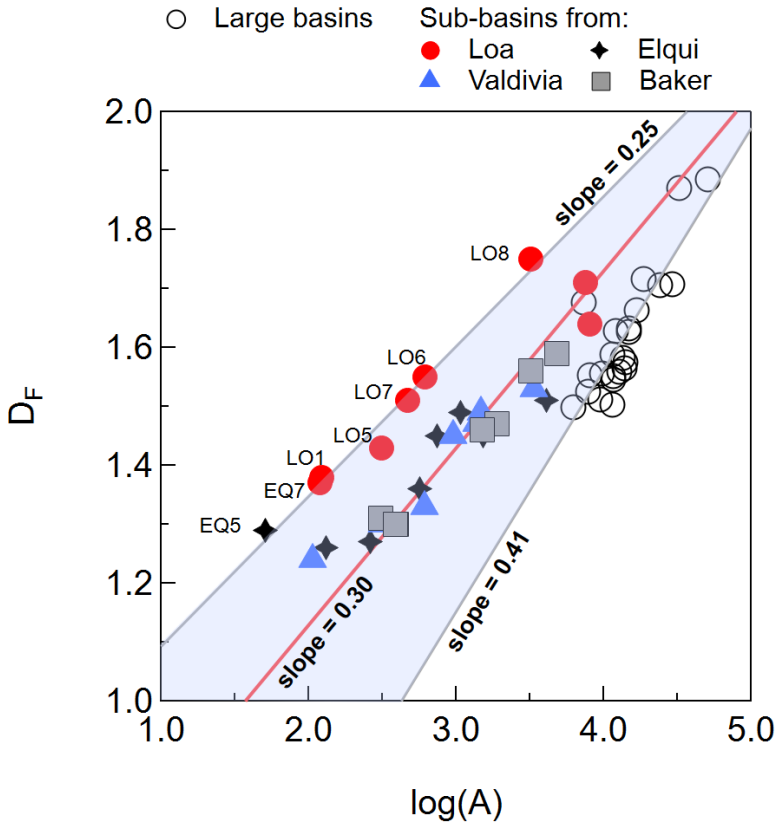

Figure 6. D_F versus $log(A)$ for large and sub-networks. Continuous lines correspond to fits $D_F \propto slog(A)$ where s is the slope of the curve ($s = 0.25, 0.30, 0.41$ for each dataset). The fit $s = 0.30$ is arbitrary.

Preprints (www.preprints.org) | NOT PEER-REVIEWED | Posted: 29 December 2021 doi:10.20944/preprints202112.0471.v1

Figure 6 compares D_F with $log(A)$ for all the units. An unexpected nice agreement was obtained between the points, with data splitting-up into three different groups. Each group can be characterized by a linear fit of slope s, that is, $s = 0.41$ for large basins, $s = 0.25$ for sub-basins $EQ5, EQ7, LO1, LO5, LO6, LO7, LO8$ and an arbitrary central fit of slope $s = 0.30$ for the rest of sub-networks. This pattern of organisation is quite surprising, considering the apparent disorganised character of Chilean territory quite well known with respect to their latitudinal development, the current and past tectonic and geomorphological processes and the factors conditioning the climatic and hydrological characteristics, all of them already discussed in sub-section 3.1. The fits proposed in Figure 6 suggest that D_F depends significantly upon network's area. Thus, we can propose the simple allometric scaling $D_F \propto s \cdot log(A) = log(A^s)$, with s an area-dependent parameter. Curiously, this fit has been also obtained from measurements of fractal dimension in urban environments(see [34]).

Figure 7 compares Fractalyse results with the analytical models detailed in section 1.1 (see Eqs.2-5). Notice that Eq.2 systematically underestimates the fractal dimension, both for large units and sub-basins. In contrast, Liu's approach (Eq.5) provides the highest values of the entire record leading, in some cases, towards values higher than 2. However, a fractal dimension higher than 2 (whatever the model used) is an unexpected result, not representative of the networks here explored. Only the model proposed by La Barbera and Rosso and Tarboton et al. (Eqs.3-4, respectively) show closeness with Fractalyse estimations, from our point of view the most representative values for our networks. The Pearson correlation index r_k was also estimated between D_k and D_F, when $k = 1, ..., 4$ (following the notation used in Eqs.2-5, obtaining $(r_2, r_3) = (0.78, 0.77)$ for large-basins and $(r_2, r_3) = (0.77, 0.55)$ at sub-basins level. Such results, confirms the agreement between Eqs.3-4 and Fractalyse, as detailed before.

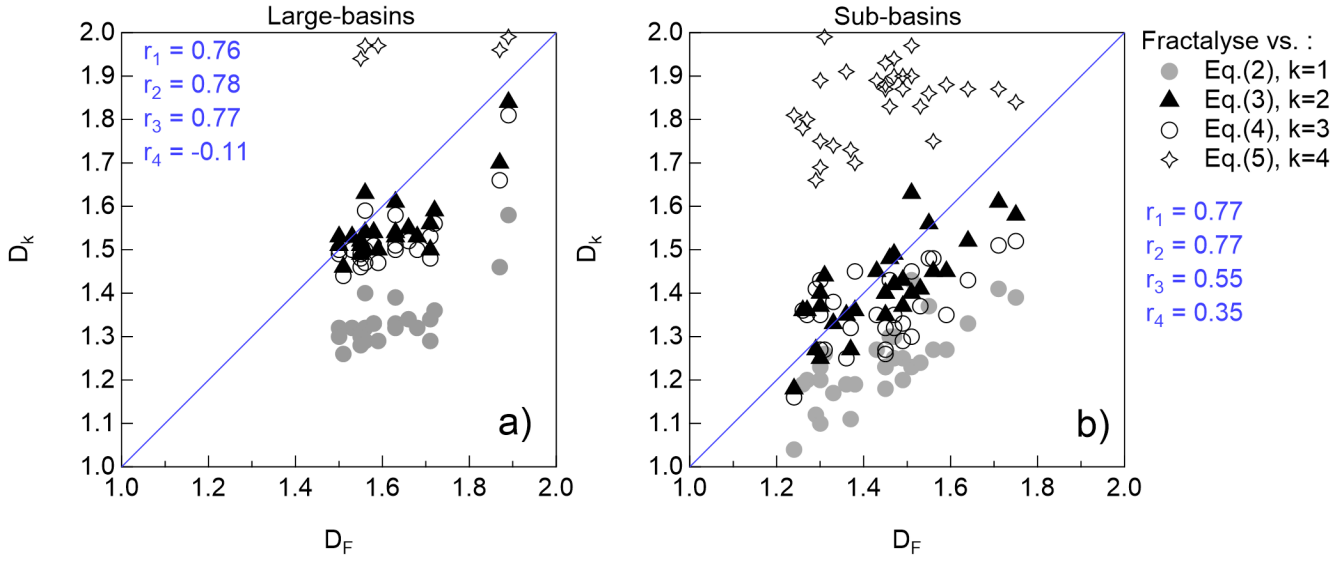

Figure 7. Comparison between Fractalyse results (D_F) and Eq.2 ($k = 1$), Eq.3 ($k = 2$), Eq.4 ($k = 3$) and Eq.5 ($k = 4$) for (**a**) large-basins and (**b**) sub-basins. The parameter r_k denotes the Pearson correlation index between the each model and Fractalyse, for $k = 1, ..., 4$.

4. Discussion

4.1. Fractal dimension: an area-dependent parameter

The curves presented in Figure 4 lead to the relationship $R_q = \xi + \eta log(A)$, with $q = A, B, L$ and ξ, η fitting parameters, with η the slope of each curve. Let's define the parameter $\zeta = \frac{log(R_p)}{log(R_q)}$, with $p = B$ and $q = L, A$. This parameter can be also written as $\zeta = \frac{log(\xi + \eta log(A))}{log(\xi' + \eta' log(A))}$, with ξ', η' another fitting parameters. The relationship between

Preprints (www.preprints.org) | NOT PEER-REVIEWED | Posted: 29 December 2021 doi:10.20944/preprints202112.0471.v1

ζ and A can be observed in Figure 8a. Referential averages of each dataset were also included ($\bar{\zeta} = 1.28$ for $q = L$ and $\bar{\zeta} = 0.96$ for $q = A$). For $q = L$ (points in red), this distribution presents a significant deviation around its average, particularly important in the range $A \geq 24,223 km^2$. Although less evident, such departure also appears for $q = A$ (points in gray), being significant in the range $A \leq 261 km^2$. Thus, an intrinsic variability of Eqs. 2-5 with A can be observed. To delve into the properties of ζ we have built the Figure 8b. In this graph, we show how large is the departure between ζ and D_F, comparing the ratio $\frac{D_F}{\zeta}$ with the A. Notice that $\frac{D_F}{\zeta}$ is always larger than unity, showing an almost linear increasing behaviour with A in the range $A < 6219 km^2$. When $A \geq 6219 km^2$, a kind of saturation effect can be observed, where $\frac{D_F}{\zeta} \approx \kappa_3$ with κ_3 a fitting parameter.

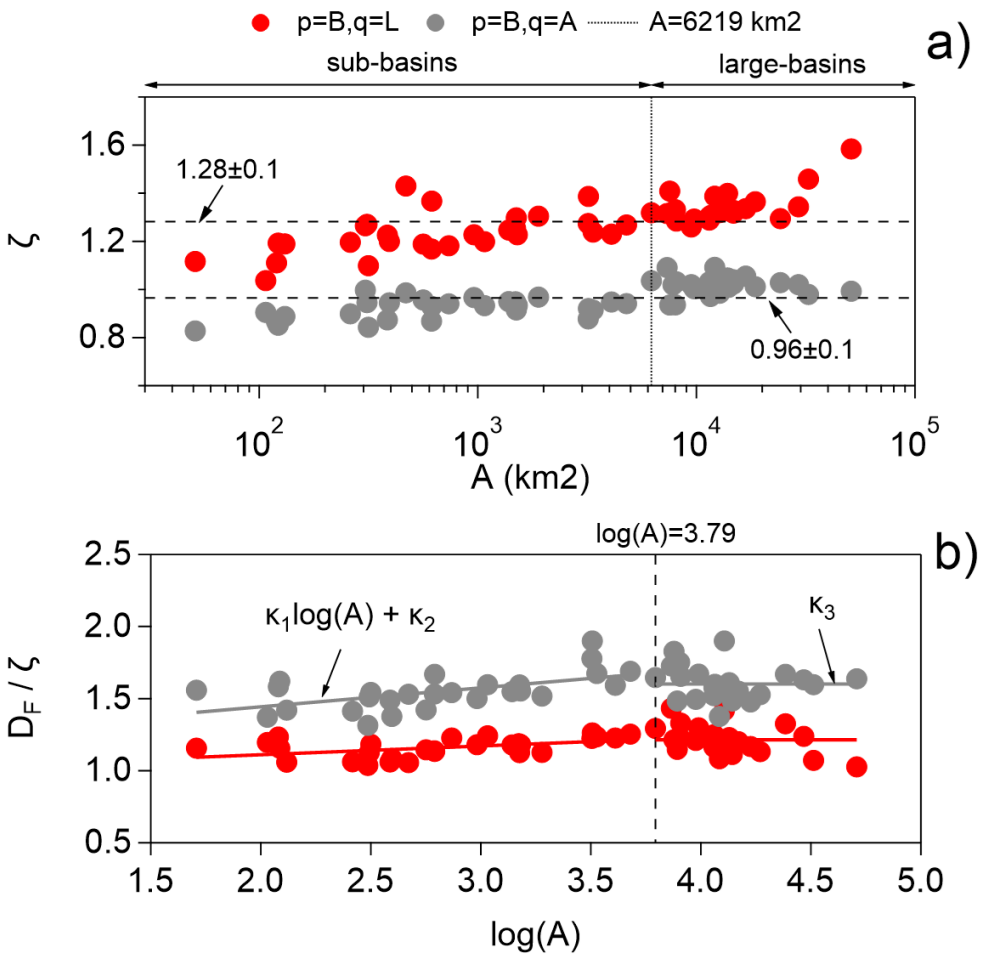

Figure 8. (**a**) Comparison between ζ and A ($p = B; q = A, L$), for large and sub-networks. The vertical line is a referential value denoting the transition area, separating both kind of networks ($A = 6219 km^2$). Horizontal dashed-lines correspond to the averages $\bar{\zeta} = 1.28$ for $q = L$ and $\bar{\zeta} = 0.96$ for $q = A$, respectively. (**b**) Comparison between the ratio D_F/ζ and $log(A)$. Continuous lines corresponds the fit proposed in Eq. 9.

Taking these elements into account, both growth regimes can be roughly described by the next relationships:

$$\frac{D_F}{\zeta} \propto \kappa_1 log(A) + \kappa_2 \quad if \quad A < 6219 km^2 \quad \& \quad \frac{D_F}{\zeta} = \kappa_3 \quad if \quad A \geq 6219 km^2 \qquad (9)$$

Preprints (www.preprints.org) | NOT PEER-REVIEWED | Posted: 29 December 2021 doi:10.20944/preprints202112.0471.v1

where $\kappa_1, \kappa_2, \kappa_3$ are fitting constants. When $q = L$ we obtain $(\kappa_1, \kappa_2, \kappa_3) = (0.06 \pm 0.02, 0.99 \pm 0.1, 1.21 \pm 0.02)$, but for $q = A$ we obtain instead $(\kappa_1, \kappa_2, \kappa_3) = (0.13 \pm 0.04, 1.18 \pm 0.1, 1.60 \pm 0.02)$. Notice that κ_1 is small, but not small enough to neglect the term $\kappa_1 log(A)$ at all. In any of both regimes, significant contrast arise when considering R_L or R_A in the determination of ζ and thus, the fractal dimension D_k for $k = 1, ...4$. Such saturation effect observed for very large areas emphasises the idea that fractal dimension of fluvial networks cannot growth indefinitely. There must be a limit for this index according to the *full-filling space* concept proposed by [24], that is, fractal dimension cannot exceed the dimension of the embedding space for this case ($D_F = 2$). These results also show that fractal values obtained from both methodologies can be related through a law of the type $D_F = \psi(A, d)D_k$, where d is the meandering fractal dimension of the mainstream and ψ a fitting function. This function shows a linear variation with A for sub-networks and $\psi \approx C^{st}$, for larger units. This area-dependence structure can be also obtained from Figure 6. At this point, it is quite important mentioning that the variability of the ramification patterns observed in our networks, are properly taken into account by a box-counting algorithm. Such characteristic is, however, not necessarily considered when the fractal dimension is only estimated from the analytical expressions based on Horton ratios. Meandering or avulsion patterns of ramification of individual streams are not always considered by a Hortonian-like structure; even more, it is not always possible to do that particularly when streams are analysed at very large scales. Then, serious differences are expected when comparing both methods of calculation as shown in Figure 8. This effect was also suggested by [35].

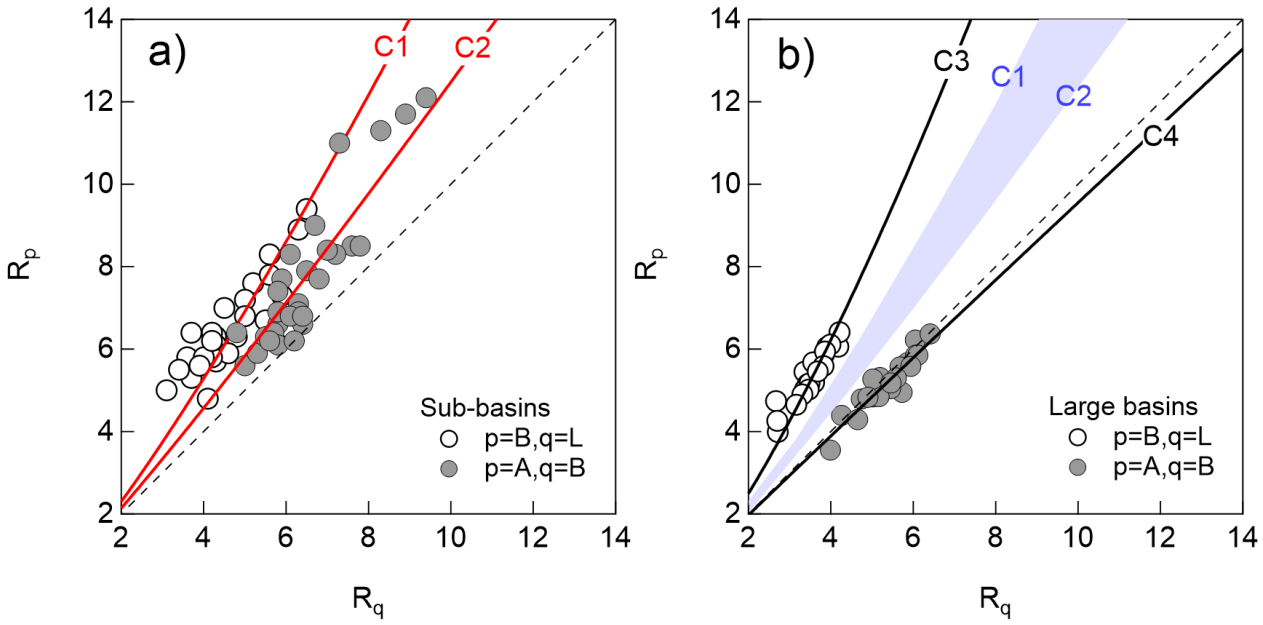

Figure 9. Comparison between R_p and R_q for (**a**) sub-basins and (**b**) large-basins measurements. Continuous lines ($C1 - C4$) correspond to power-law fits of the form $R_p = R_q^m$, where m is a fitted exponent for each dataset.

In the same context, a comparison between the Horton parameters calculated for all the units can be observed in Figures 9a-9b. As anticipated by Figure 4, patterns of regularity also arise in this case. Such regularity is quite evident for large-basins measurements, and less evident for sub-network measurements. In any of both cases, both distributions can be roughly described by a law of the type $R_p = {R_q}^m$ $(p \neq q)$, with m a characteristic exponent of each curve. For sub-networks we obtain $m = 1.20$ for $p = B, q = L$ (fit C1) and $m = 1.09$ for $p = A, q = B$ (fit C2). In contrast, for large-networks measurements we get $m = 1.32$ for $p = B, q = L$ (fit C3), whereas $m = 0.98$ for $p = A, q = B$ (fit C4). By one hand, these exponents show that Horton ratios measured at sub-basin level are strictly bounded by large watersheds data but on the other side,

Preprints (www.preprints.org) | NOT PEER-REVIEWED | Posted: 29 December 2021 doi:10.20944/preprints202112.0471.v1

these metrics are dependent on the size of the units, even if they were extracted from the same morphological unit. Once again, this area-dependent character can be observed in many parameters at the same time revealing that fluvial networks analysed in this paper are objects whose behaviour is far from "pure" fractals typically reported in literature.

Another striking element arises when analysing sub-networks from the North of the country. In this case, dataset shows an important dispersion suggesting the influence of tectonics control in our measurements, particularly when we discuss about this scale-invariance property. This competition between tectonics and water-erosive effects have been discussed by [36] and it is inherent to the fractal dimension of a fluvial network. Soil characteristics, lithology and tectonic conditions are major agents of influence on the final pattern of a fluvial network. However, climatic and hydrological conditions play a sculpting role on a given network, influencing the measure of its fractal properties. If we analyse the role played by other geomorphic parameters, Figure 5a shows however no clear trends, for example, between D_F and the mean slope i_m or the drainage density ρ (Figures 5a-5b). In this last case, however, D_F strongly concentrates in the range $0.8 < \rho < 1.24$, slightly increasing for higher drainage densities. This effect becomes more clear for networks under the influence of Nazca North segment-plate (*e.g. LO* and *QC*), showing an accentuated contrast with the basins from the rest of the country. Following this idea, it is equally surprising that sub-basin dataset, in almost all the cases, shows a tendency to group in regimes different from those observed for larger units. This departure could be explained because of the detailed morphological information obtained at a finer measurement scale, not possible to recover when analysing the same morphological unit with a larger "ruler".

Our results also shows that the determination of the fractal dimension is quite sensitive to the choice of the method of calculation. From an analytical point of view, if Eq. 2 approach underestimates this parameter, Eq.4 over-estimates it leading to unrealistic values larger than 2 (the theoretical limit for our networks). The approach proposed by Tarboton et al. (Eq.3) it is the only model presenting a rough agreement with Fractalyse results (see Figure 7). Thus, the models given by Eqs.3-5 a size-dependent multiplicative factor should be involved and therefore, the universality of such formulations must be carefully analysed. Claps and Oliveto [35] seems to support this idea, proposing a size-dependent coefficient on the allometric relationships of a given basin. Following this argument, we wonder to which extent the fractal dimension of a large-basin could be reproduced by averaging the fractal dimensions of their respective sub-basins. According to our measurements, the closeness (or distance) between these results could be interpreted as a sign of self-similarity patterns related to the distribution of the fractal dimension of each network, in particular for Loa, Elqui,Valdivia and Baker. Among the many ways to perform such averaging, here we have considered an area-weighed law for such purpose, that is:

$$\bar{D}_i = \frac{D_1 A_1 + ... + D_{n(i)} A_{n(i)}}{A_1 + ... + A_{n(i)}} \tag{10}$$

where $\bar{D}_i$ is the average value of the sub-networks extracted from a given large-basin, for $i = 1, ..., 4$, ($i = 1$ for Loa, $i = 2$ for Elqui, $i = 3$ for Valdivia and $i = 4$ for Baker); $n(i)$ is the number of such sub-basins and A_k the area of each of them ($k = 1, ..., n(i)$). The parameter D_k corresponds to the fractal dimension of the sub-networks already estimated by the methods detailed in Eqs. 2-6. Table 4 shows a comparison of $\bar{D}_i$. The calculations evidence clear discrepancies between the results, suggesting *a priori* the impossibility of recovering the fractal dimension of the entire basin by simply averaging the fractal values of its "parts", whatever the model used. Only when comparing Fractalyse results, the regions of Elqui and Valdivia show some similarities. From our point of view, this result emphasizes the idea that Chilean networks cannot be considered strictly as self-similar systems, being quite sensitive to the choice of the model of estimation.

Preprints (www.preprints.org) | NOT PEER-REVIEWED | Posted: 29 December 2021 doi:10.20944/preprints202112.0471.v1

Table 4. Averaged fractal dimension $\bar{D}_k$ for Loa ($k = 1$), Elqui ($k = 2$), Valdivia ($k = 3$) and Baker ($k = 4$) basins, calculated according to different models. Fractalyse values were also included for comparison. Values of the entire basin are shown in the last column, obtained from the Table 3.

Averages for	When D_k is calculated from:					Dimension of the entire basin
sub-basins from:	Eq.2	Eq.3	Eq.4	Eq.5	Fractalyse	Fractalyse
Loa ($\bar{D}_1$)	1.37	1.56	1.47	1.87	1.67	1.89
Elqui ($\bar{D}_2$)	1.22	1.39	1.30	1.88	1.47	1.51
Vadivia ($\bar{D}_3$)	1.23	1.40	1.34	1.85	1.48	1.50
Baker ($\bar{D}_4$)	1.27	1.46	1.39	1.85	1.52	1.71

4.2. About the relationship between ρ, A, i_m and the fractal dimension of each network.

From the results presented though this paper is clear that a relationship between the mean slope, the drainage density and the fractal dimension of each network must exists. Such interplay can be observed in Figure 10. Climatic and tectonics effects on data were also qualitatively indicated in the same graph.

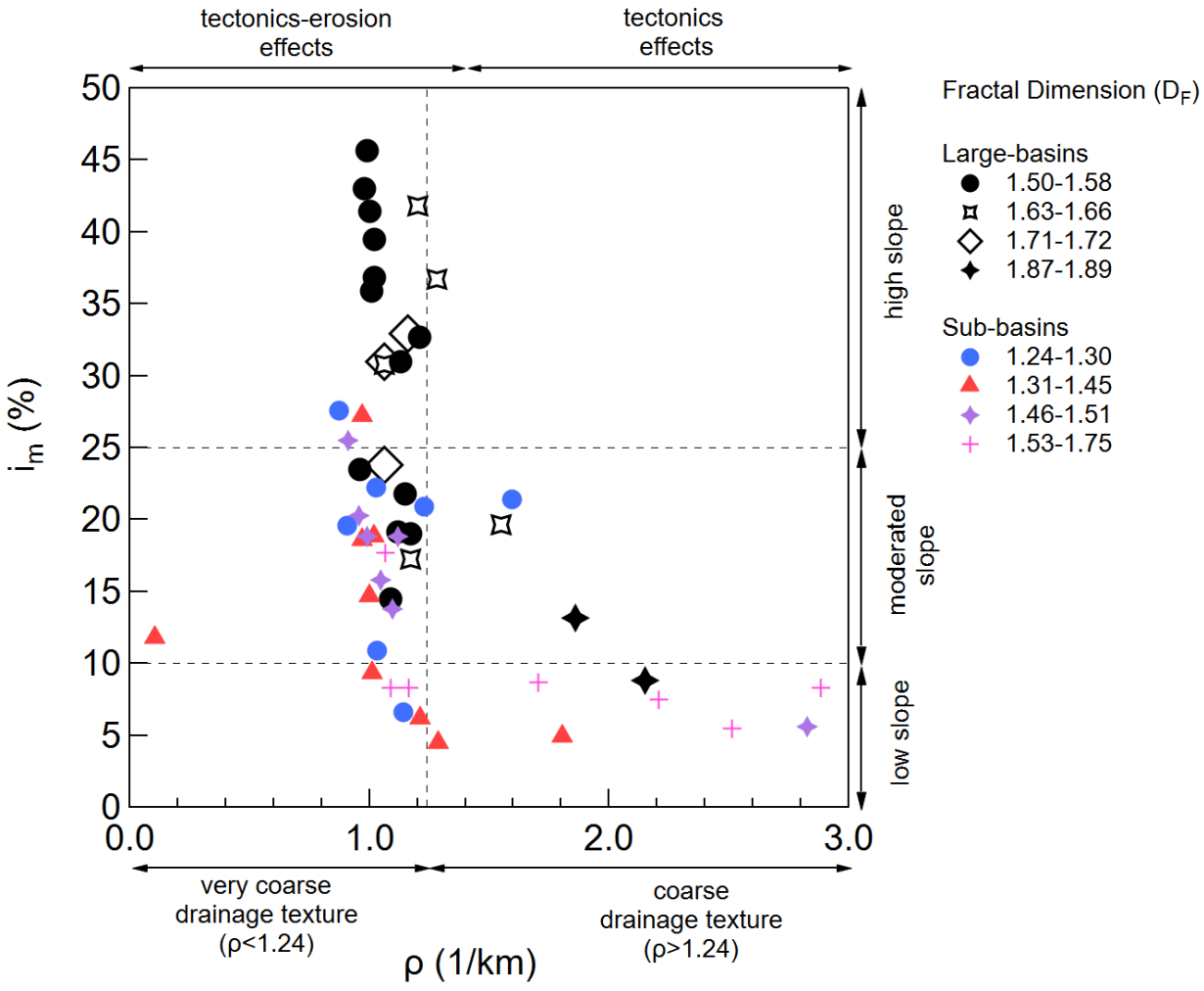

Figure 10. Diagram between ρ, the mean slope i_m, the fractal dimension and the dominant tectonics and climatic conditions.

 doi:10.20944/preprints202112.0471.v1

About this diagram it is important to introduce two elements. First, the subduction influence of Nazca and Antarctic plates shows a west-east direction, also known as the *collision margin* with the South American plate. Such phenomenon has generated the main morphostructural units organized in longitudinal bands of the relief already explained in Section 3.1. Second, in general the development of the different climatic types is related with the global atmospheric circulation patterns, allowing a latitudinal climatic zonification in the north-south direction. For this reason, arid climates in the north progressively becomes more humid towards the south of the country. From these considerations, it is reasonable to think about isolated or combined natural effects in the development of drainage networks. In this context, most of fluvial networks in Chile have been the combined result of both, tectonics and erosive processes, giving rise to very coarse drainage textures ($\rho < 1.24$), with a tendency to present moderate to high slopes in larger basins (for which fractal values falls in the range $1.50 \leq D_F \leq 1.72$) and moderate to low slopes sub-basins (with values in the range $1.24 \leq D_F \leq 1.51$). On the other hand, a smaller sub-set of basins shows a strong tectonics influence on their drainage patterns, only because of they are located in the north of the country. These units present moderate to low slopes regimes and coarse drainage textures ($\rho \geq 1.24$), for which fractal values are essentially high ($1.87 \leq D_F \leq 1.89$ for large-basins and $1.53 \leq D_F \leq 1.75$ for sub-networks). This level of organisation is not coincidental, revealing a non-aleatory connection between tectonics, climate and fractality, questioning this apparent disordered character of the territory.

5. Conclusions

In this paper we have studied the fractal properties of Chilean relief by measuring morphometric properties of fluvial networks distributed across the country, analysed at different scales. The mono-fractal dimension of each unit was estimated by applying two different methods: one, based on Horton ratios metrics and another one, based on a box-counting algorithm trough Fractalyse. A first impression is that such estimations are quite sensitive to the chosen method, revealing significant differences at sub-basin level. In this sens, only the approaches proposed by Eq.3 and Eq.4 show similarities with Fractalyse data, suggesting that a box-counting method seems to better captures the main topological features of each network (*e.g.* the shape of individual streams, the presence of curvatures, meanders and avulsion patterns, among others). Such features are essentially a consequence of the erosive power of the streams, as well as by structural control whose influence is visible throughout Chilean territory.

Following this argument, fractal dimension estimated from Fractalyse (D_F) for large-basins located under the influence of the Nazca North segment show values in the range $1.66 \leq D_F \leq 1.89$, while networks located in Antartica plate fall in the range $1.63 \leq D_F \leq 1.71$. Both ranges evidence a clear contrast between the extreme regions of the country. On the other side, basins located under the influence of Nazca Flat Slab and Nazca South segments fall in the range $1.50 \leq D_F \leq 1.72$. These last values are close to the magnitudes reported in the cited literature, particularly for networks developing on alluvial fans like the morpho-structural unit *Central Depression* detailed in Section 3.1. It is also interesting mention that these basins are influenced by Mediterranean climates. These latitudinal differences emphasises, once again, the structural control on the ability of a fluvial network to diffuse into the basin. Such effects introduce morphological anisotropic features on drainage patterns, as suggested by [24]. This characteristic is present in most of networks analysed in this report and is intimately related with the concept of *self-affine* diffusion of streams.

Analyzing this information at sub-basin level, the results becomes as surprising, as disturbing. Fractal values for these units show a clear departure with respect to the values observed at larger units. This is the case of Loa, Elqui, Valdivia and Aysen. Such departure is strongly revealed when looking at the distribution of Horton ratios and geomorphic indexes as well (F, C, E). Despite these differences, reasonable groupings

between D_F and the size of each unit were obtained (see Figure 6), conducting to nice correlations of the type $D_F \propto slog(A)$, with s an area-dependent exponent. A similar conclusion was obtained from Figure 8b. This result suggest that D_F should not be considered a scale-invariant parameter, but rather a complex function of the are of the network, and the meandering pattern of diffusion of individual streams. landscape. This kind of connection between fractal dimension and the area of the object was reported previously by [34] from measurements on urban environments.

Finally, all the results presented in this paper invite to consider the fractal dimension as a rich geomorphic parameter revealing the self-affine character of fluvial networks as inferred from the the results presented in Table 4. This parameter could definitely help to improve our comprehension about the characteristics of drainage patterns measured across the territory. The information provided by this dimension is no possible to get from classical morphometric indexes (*e.g.* parameters F, C, E). In this context, it is very surprising that despite the climatic, morphological, tectonic and lithological variability of the country, a significant amount of parameters show reasonable groupings and trends (*e.g.* Figures 6,9,10). These striking patterns of organisation seems to be camouflaged into each basin, inviting to consider Chilean territory not as so "crazy", nor so unpredictable as believed.

Chilean landscapes could be taken as a powerful natural laboratory to test the validity of mprphometric and fractal scaling-laws, widely disseminated in the literature (*e.g.* Eqs.2-5). Most of these findings deserve to be analysed with more detail, but due to the scale of such work it requires to use a methodology different from that reported here. In this context, a multifractal analysis is an interesting tool to conduct this process considering the complex mechanisms involved on the generation and evolution of a fluvial network. This is a very challenging task will definitely be the goal of a next report.

Author Contributions: Conceptualization,FM; methodology, FM,HM,AO; formal analysis,FM,HM; investigation,FM,HM,AO,GO; data curation,AO,GO; writing/original draft preparation, FM; writing/review and editing, FM,HM; supervision, FM; project administration, FM. All authors have read and agreed to the published version of the manuscript.

Funding: This research received no external funding

Acknowledgments: The authors thank to the School of Civil Engineering from the Pontificia Universidad Catolica de Valparaiso (PUCV) for the support given to conduct this study.

Conflicts of Interest: The authors declare no conflict of interest

Appendix A Drainage patterns of sub-networks

In this appendix we can observe the drainage patterns of the 33 sub-basins extracted from Loa ($LO1 - LO8$), Elqui ($EQ1 - EQ7$), Valdivia ($VA1 - VA7$) and Baker ($BA1 - BA7$) watersheds.

Preprints (www.preprints.org) | NOT PEER-REVIEWED | Posted: 29 December 2021 doi:10.20944/preprints202112.0471.v1

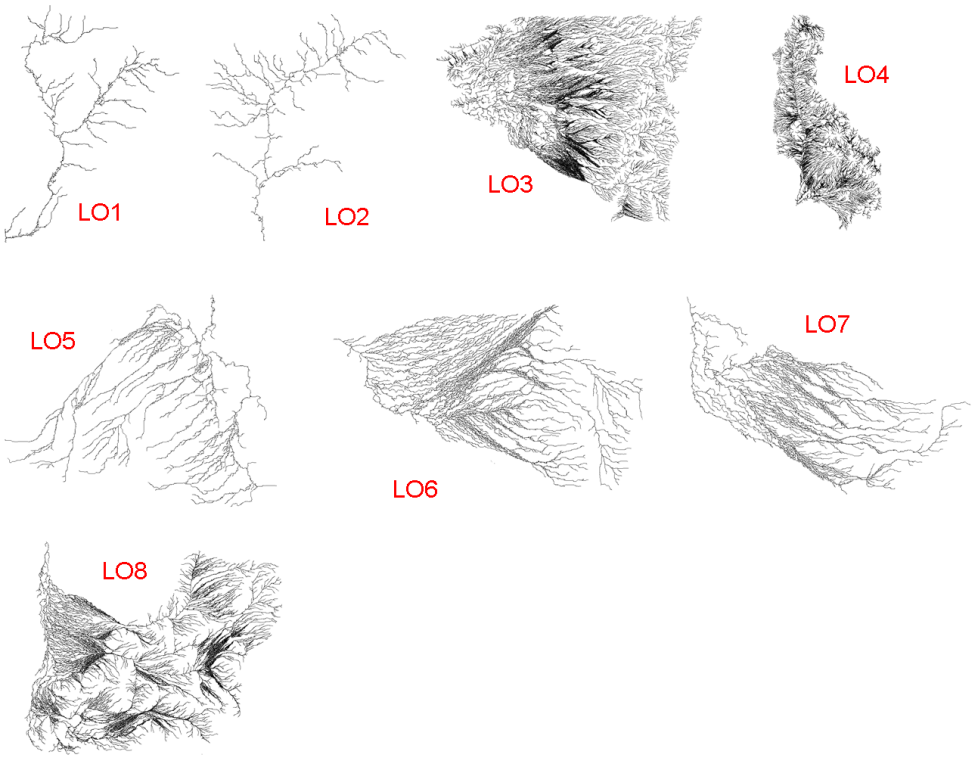

Figure A1. Drainage networks extracted from Loa basin.

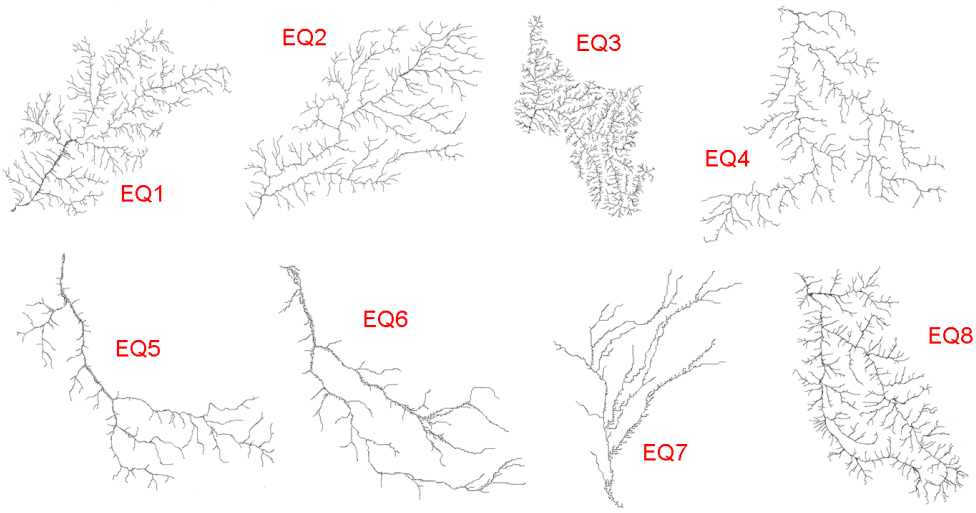

Figure A2. Drainage networks extracted from Elqui basin.

Preprints (www.preprints.org) | NOT PEER-REVIEWED | Posted: 29 December 2021 doi:10.20944/preprints202112.0471.v1

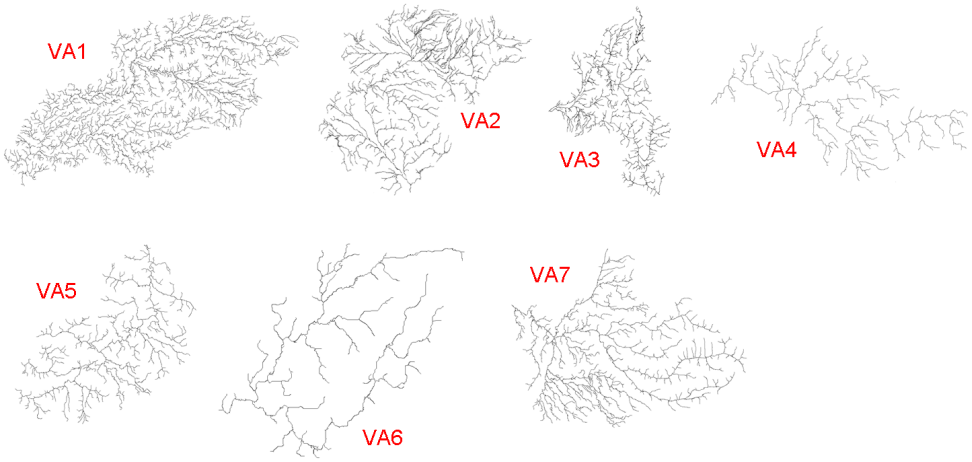

Figure A3. Drainage networks extracted from Valdivia basin.

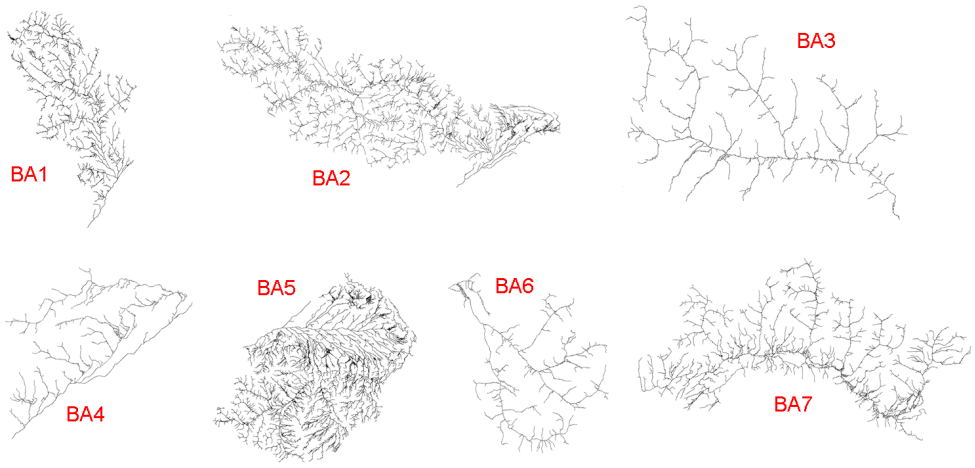

Figure A4. Drainage networks extracted from Baker basin.

References

1. Mandelbrot, B.B.; Mandelbrot, B.B. *The fractal geometry of nature*; Vol. 1, WH freeman New York, 1982.
2. La Barbera, P.; Rosso, R. On the fractal dimension of stream networks. *Water Resources Research* **1989**, *25*, 735–741.
3. Tarboton, D.G.; Bras, R.L.; Rodriguez-Iturbe, I. The fractal nature of river networks. *Water Resources Research* **1988**, *24*, 1317–1322.
4. Turcotte, D.L. Fractals in geology and geophysics. *Pure and Applied Geophysics* **1989**, *131*, 171–196.
5. Gregory, K.; Gregory, P.; Walling, D. *Drainage Basin Form and Process: A Geomorphological Approach*; Wiley, 1973.
6. Feder, J. *Fractals*; Physics of Solids and Liquids, Plenum Press, 1988.
7. Subercaseaux, B. *Chile o una loca geografía*; Editorial Universitaria, 2005.
8. Horton, R.E. Erosional development of streams and their drainage basins; hydrophysical approach to quantitative morphology. *Geological society of America bulletin* **1945**, *56*, 275–370.
9. Chow, V. *Applied Hydrology*; McGraw-Hill Series in Water Resources and Environmental Engineering, Tata McGraw-Hill Education, 2010.
10. Tokunaga, E. Consideration on the composition of drainage networks and their evolution. *Geographical Reports of Tokyo Metropolitan University* **1978**, *13*, 1–27.
11. Tarboton, D.G. Fractal river networks, Horton's laws and Tokunaga cyclicity. *Journal of Hydrology* **1996**, *187*, 105–117.
12. Hack, J.T. *Studies of longitudinal stream profiles in Virginia and Maryland*; Vol. 294, US Government Printing Office, 1957.
13. Rosso, R.; Bacchi, B.; La Barbera, P. Fractal relation of mainstream length to catchment area in river networks. *Water Resources Research* **1991**, *27*, 381–387.
14. Liu, T. Fractal structure and properties of stream networks. *Water Resources Research* **1992**, *28*, 2981–2988.

15. Tarboton, D.G.; Bras, R.L.; Rodriguez-Iturbe, I. Comment on "On the fractal dimension of stream networks" by Paolo La Barbera and Renzo Rosso. *Water Resources Research* **1990**, *26*, 2243–2244.
16. Tarboton, D.G.; Bras, R.L.; Rodriguez-Iturbe, I. Scaling and elevation in river networks. *Water Resources Research* **1989**, *25*, 2037–2051.
17. Schuller, D.; Rao, A.; Jeong, G. Fractal characteristics of dense stream networks. *Journal of Hydrology* **2001**, *243*, 1–16.
18. La Barbera, P.; Rosso, R. Reply [to "Comment on 'On the fractal dimension of stream networks' by Paolo La Barbera and Renzo Rosso"]. *Water Resources Research* **1990**, *26*, 2245–2248, [https://agupubs.onlinelibrary.wiley.com/doi/pdf/10.1029/WR026i009p02245]. doi:https://doi.org/10.1029/WR026i009p02245.
19. Kirchner, J.W. Statistical inevitability of Horton's laws and the apparent randomness of stream channel networks. *Geology* **1993**, *21*, 591–594.
20. Nikora, V.I.; Sapozhnikov, V.B. River network fractal geometry and its computer simulation. *Water Resources Research* **1993**, *29*, 3569–3575.
21. Nikora, V.I.; Sapozhnikov, V.B.; Noever, D.A. Fractal geometry of individual river channels and its computer simulation. *Water Resources Research* **1993**, *29*, 3561–3568.
22. Nikora, V.I. On self-similarity and self-affinity of drainage basins. *Water Resources Research* **1994**, *30*, 133–137.
23. Dodds, P.S.; Rothman, D.H. Scaling, universality, and geomorphology. *Annual Review of Earth and Planetary Sciences* **2000**, *28*, 571–610.
24. Phillips, J. Interpreting the fractal dimension of river networks. *Fractals in Geography* **1993**, *7*, 142–157.
25. Frankhauser, P. Fractal geometry for measuring and modelling urban patterns. In *The dynamics of complex urban systems*; Springer, 2008; pp. 213–243.
26. Thomas, I.; Frankhauser, P.; Badariotti, D. Comparing the fractality of European urban neighbourhoods: do national contexts matter? *Journal of Geographical Systems* **2012**, *14*, 189–208.
27. Rodriguez-Iturbe, I.; Rinaldo, A. *Fractal river basins: chance and self-organization*; Cambridge University Press, 2001.
28. Strahler, A.N. Hypsometric (area-altitude) analysis of erosional topography. *Geological Society of America Bulletin* **1952**, *63*, 1117–1142.
29. Dorsaz, J.M.; Gironás, J.; Escauriaza, C.; Rinaldo, A. The geomorphometry of endorheic drainage basins: implications for interpreting and modelling their evolution. *Earth Surface Processes and Landforms* **2013**, *38*, 1881–1896.
30. Charrier, R.; Pinto, L.; Rodríguez, M.P. Tectonostratigraphic evolution of the Andean Orogen in Chile. In *The Geology of Chile*; Geological Society of London, 2007. doi:10.1144/GOCH.3.
31. Anderson, R.S.; Anderson, S.P. *Geomorphology: the mechanics and chemistry of landscapes*; Cambridge University Press, 2010.
32. Moreno, T.; Gibbons, W. *The Geology of Chile*; Geological Society of London, 2007. doi:10.1144/GOCH.
33. Donadio, C.; Magdaleno, F.; Mazzarella, A.; Kondolf, G.M. Fractal dimension of the hydrographic pattern of three large rivers in the Mediterranean morphoclimatic system: geomorphologic interpretation of Russian (USA), Ebro (Spain) and Volturno (Italy) fluvial geometry. *Pure and Applied Geophysics* **2015**, *172*, 1975–1984.
34. Shen, G. Fractal dimension and fractal growth of urbanized areas. *International Journal of Geographical Information Science* **2002**, *16*, 419–437, [https://doi.org/10.1080/13658810210137013]. doi:10.1080/13658810210137013.
35. Claps, P.; Oliveto, G. Reexamining the determination of the fractal dimension of river networks. *Water Resources Research* **1996**, *32*, 3123–3135.
36. Turcotte, D.L. Fractal tectonics and erosion. *Fractals* **1993**, *1*, 491–512.